On Realizing Higher Efficiency Polymer Solar Cells Using a Textured Substrate Platform

*Kanwar S. Nalwa, Joong-Mok Park, Kai-Ming Ho, and Sumit Chaudhary**

Organic photovoltaic (OPV) technology is an attractive solar-electric conversion paradigm due to the promise of low cost roll-to-roll production and amenability to flexible substrates. Substantial progress has been made over the last 5 years, by virtue of optimization of materials processing parameters[1–3] and emergence of new conjugated polymers with tailored energy levels.[4–6] Power conversion efficiency (PCE) exceeding 7% has recently been achieved.[4] The state-of-the-art devices are so called bulk-heterojunction (BHJ) type in which the PV active-layer is coated from a blend of donor and acceptor species. The nanoscale nature of phase separation between the donors and acceptors in a BHJ active-layer alleviates the mismatch between exciton diffusion length (~10 nm) and optical absorption length (>100 nm). However, there still exists a mismatch between optical absorption length and charge transport scale. BHJ active-layers tend to suffer from cul-de-sacs in the charge transport pathways, and hole mobilities in conjugated polymers remain low. Both of these factors lead to recombination losses, higher series resistances and lower fill-factors.[7] Thus, it is imperative to develop fabrication methodologies that can enable efficient optical absorption in films thinner than optical absorption length. The most desirable methodology would be one which can also substantially improve absorption at the band edge of conjugated polymers, which usually lies in the red/near-infrared region, and where significant amount of solar flux is also located. It is more so important because the charge carriers photoexcited at the band edge were found to have a higher dissociation efficiency than the ones excited at higher energies.[8] Textured substrate based light-trapping schemes are a commonplace in traditional inorganic photovoltaic (PV) cells. However, they have not been successfully applied to polymer based PVs due to an obvious problem of solution-processing nanoscale thick and conformal PV layers on topographical surfaces. In this communication, we show that realization of such conformal layers is indeed possible, if the underlying topography has suitable dimensions. We fabricated poly(3-hexylthiophene): [6,6]-phenyl-C61-butyric acid methyl ester (P3HT:PCBM) based BHJ PV cells on grating-type textured substrates possessing several sub-micrometer and micrometer scale topographical dimensions. We discovered that if the height of the underlying topographical features is reduced to sub-micrometer regime (e.g. 300 nm) and the pitch is increased to more than a micrometer (e.g. 2 μm), the textured surface becomes amenable to coating a conformal PV active-layer. The resultant PV cells showed 100% increase in average light absorption near the band edge due to trapping of higher wavelength photons, and 20% improvement in PCE as compared with the flat PV cell.

Till date, a few light management techniques in ray optics regime have been investigated for enhancement of optical absorption in OPVs, namely, collector mirrors,[9] and a macroscale configuration in which two OPV cells were mounted together in V-shape.[10] Light-trapping schemes based on periodic patterning were also reported using buried nanoelectrodes,[11] microprism substrates,[12] and azopolymer based sub-micrometer topography substrate.[13] Although enhancement in optical absorption was demonstrated in these patterning schemes, efficient OPV cells could not be realized due to processing bottlenecks. Another type of light management approach reported was embossing of active-layer to induce a sub-micrometer scale texture on an otherwise flat film.[14–16] Although the embossing approach did lead to improvement in PCE of OPV cells, the approach suffers from some drawbacks. Firstly, embossing is done at an elevated temperature. Such an annealing step is not universally desirable for all BHJ materials and can lead to degradation.[6] Secondly, the embossing step poses contamination concerns, which can lead to Schottky barrier formation at the organic/metal interface.[17] Lastly and most importantly, embossing produces alternating thick and thin regions within the PV active-layer, which is not the most optimal configuration from the point of view of charge transport, as the thicker regions are still bound to suffer from recombination losses. In this respect, we believe that a nanoscale thick active-layer uniformly or conformally coated on an underlying textured substrate (electrode) is a more promising light management paradigm than embossing. Besides light management, a textured PV cell can also enable an additional functionality of self-cleaning, which requires nanoscale roughness for superhydrophobicity.[18] Such a textured substrate paradigm, however, has not been successful in polymer based PVs due to an obvious challenge of processing such conformal films from solution. Attempts to spin-coat PV active-layer on textured substrates led to over filling of the valleys and shunts at the crests,[11,12] which severely affected the device performance. Thus, the issue of design of textured substrates for light-trapping in polymer PVs, should not solely be approached from

K. S. Nalwa, Prof. S. Chaudhary
Department of Electrical and Computer Engineering,
and Microelectronics Research Center
Iowa State University
Ames, IA 50011, USA
E-mail: sumitc@iastate.edu
Dr. J.-M. Park, Prof. K.-M. Ho
Ames Laboratory-USDOE & Department
of Physics and Astronomy
Iowa State University
Ames, IA 50011, USA

DOI: 10.1002/adma.201002898

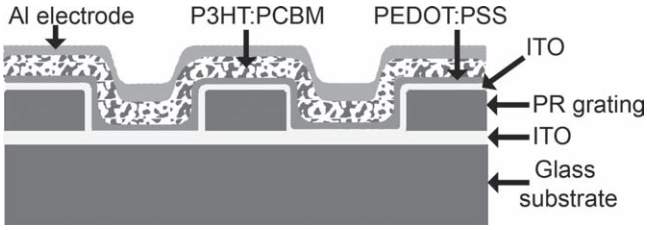

Figure 1. Schematic of the textured substrate based P3HT:PCBM solar cell.

the point of view of discovering the best optical design. Instead, we argue that an equally critical question to ask is: Which design is most amenable for realizing a conformal active-layer film from solution processing?

In this Communication, we demonstrate that it is indeed possible to realize conformal active-layers on light-trapping textured substrates, and thus higher efficiency OPVs, if the topographical dimensions of textured substrates are carefully chosen. In this study, spin-coating was used for depositing the active-layer. However, the so called suitable topographical dimensions discovered in our study should be equally relevant for realizing conformal coatings using roll-to-roll techniques like gravure coating. **Figure 1** shows the schematic of our textured substrate based devices. For this study, we used laser interference lithography to pattern photoresist in a one-dimensional diffraction grating pattern. In principle, one can also make a two-dimensional pattern, and use soft-lithography[19] or self-assembly[20] based approaches for pattern fabrication. Figure 1 is just a representative of the sequence of layers in our devices. Exact morphology of active-layer on a grating is obviously a strong function of the underlying topographical dimensions.

To evaluate the feasibility of achieving the proposed conformal layer, we investigated the gratings of several topographical dimensions. **Figure 2** shows the fate of spin-coating P3HT:PCBM active-layer on these gratings. For microscale patterns, where both pitch and height of the grating structure are greater than 1 μm, the active-layer was highly non-conformal (Figure 2a–c). There was excess polymer in the valleys and polymer-less regions at the crests that are expected to cause shunts in the final device, similar to previous reports.[11,12] Several air-gaps were also observed within the polymer film inside the valleys. Even after tailoring various spin coating parameters, conformal polymer coating could not be achieved. Intuitively, one can hypothesize that it is microscale height of the grating that led to the case of underfill and air-gaps for these samples. Thus, we resorted to gratings with sub-micrometer heights. We chose 300 nm as an exemplary sub-micrometer dimension for the height. For pitch, we chose several dimensions – 600 nm, 800 nm, and 1 μm. Figure 2d–f show the fate of spin coating P3HT:PCBM film on the grating of 300 nm height and 600 nm pitch. Quality of the polymer film improved as compared with the case of microscale height and pitch. No shunt points or air-gaps were observed. However, the film was still not conformal to the underlying topography. Valleys had more polymer than the crests, which we call the case of overfill. This excess polymer in the valleys can be expected to lead to recombination losses and poor performance. Similar overfill case was observed for the PR grating of 800 nm pitch and 1μm pitch (see supporting information). However, a clear trend in morphology was observed as the pitch increased from 600 nm to 1 μm, with amount of overfilling reducing as pitch increased. As a logical next step, we decided to increase the pitch of the grating to 2 μm while keeping the height at 300 nm. As the SEM, AFM and schematic images of Figure 2g–i reveal, these dimensions indeed enabled the realization of a uniformly thick P3HT:PCBM film that conformally followed the topography of the substrate. Thickness of the active-layer inside the valleys was identical to the thickness on the crests, as evident by the AFM height scale of 300 nm (Figure 2h). Also, no shunt-like defects were observed.

To investigate the effect of texturing on the final devices, we characterized our OPV devices based on the aforementioned textured substrates, along with a flat control. **Figure 3**[21] shows the current-voltage (I–V) characteristics of our devices. Results of devices fabricated on the microscale topography (2 μm pitch and 2 μm height) are not shown as the device failed to show PV behavior due to large number of shunts discussed above. Figure 3 shows that the conformal coating of P3HT:PCBM on the 2 μm pitch and 300 nm height substrate led to 20% increase in short circuit current density (J_{sc}) as compared with the flat control. PCE also increased by 20% since the open circuit voltage (V_{oc}) and fill-factor (FF) were not affected. V_{oc} and FF not being affected is another signature of the conformal nature of active-layer coating, because excess polymer in the grating valleys and/or shunts would have had a direct negative impact on both V_{oc} and FF. On the other hand, the overfill case of smaller pitches discussed above led to greater recombination losses in the active-layer aggregated in the valleys of the grating and the performance of the PV cells degraded in all respects (J_{sc}, V_{oc} and FF) as compared with the flat control. See supporting information for dark I–V characteristics and more discussion on V_{oc}.

In order to elucidate the light-trapping nature of our textured device platform, we did external quantum efficiency (EQE) and reflection measurements on our highest efficiency grating cell (300 nm height and 2 μm pitch) and the reference flat cell (**Figure 4**). Optical microscopy image in Figure 4a depicts a visual signature of light diffraction that occurs in grating cells when incident light is reflected back from the Al cathode. Figure 4b shows the total and scattered (higher order excluding zeroth order) reflection measured at normal incidence. Total reflection is significantly suppressed in the case of the grating PV cell. Smoother total reflection curve for grating cell indicates reduction in inference oscillations, suggesting that very little light escapes the cell after reflection from the Al cathode. As a result of negligible transmission, the reflection (R) yields an approximation to the absorption (A) using $A = 100–R$. Although the grating cell shows broadband absorption enhancement, the enhancement is much stronger for higher wavelengths, with 2.6 times enhancement at 640 nm. This enhancement is reflected in the significantly improved EQE for $\lambda > 550$ nm (Figure 4c), and further supported by higher scattered reflection from the grating cell for $\lambda > 550$ nm (Figure 4b). Due to the periodic structure of the Al cathode, incident light reaching it can be diffracted backward according to the following equation:

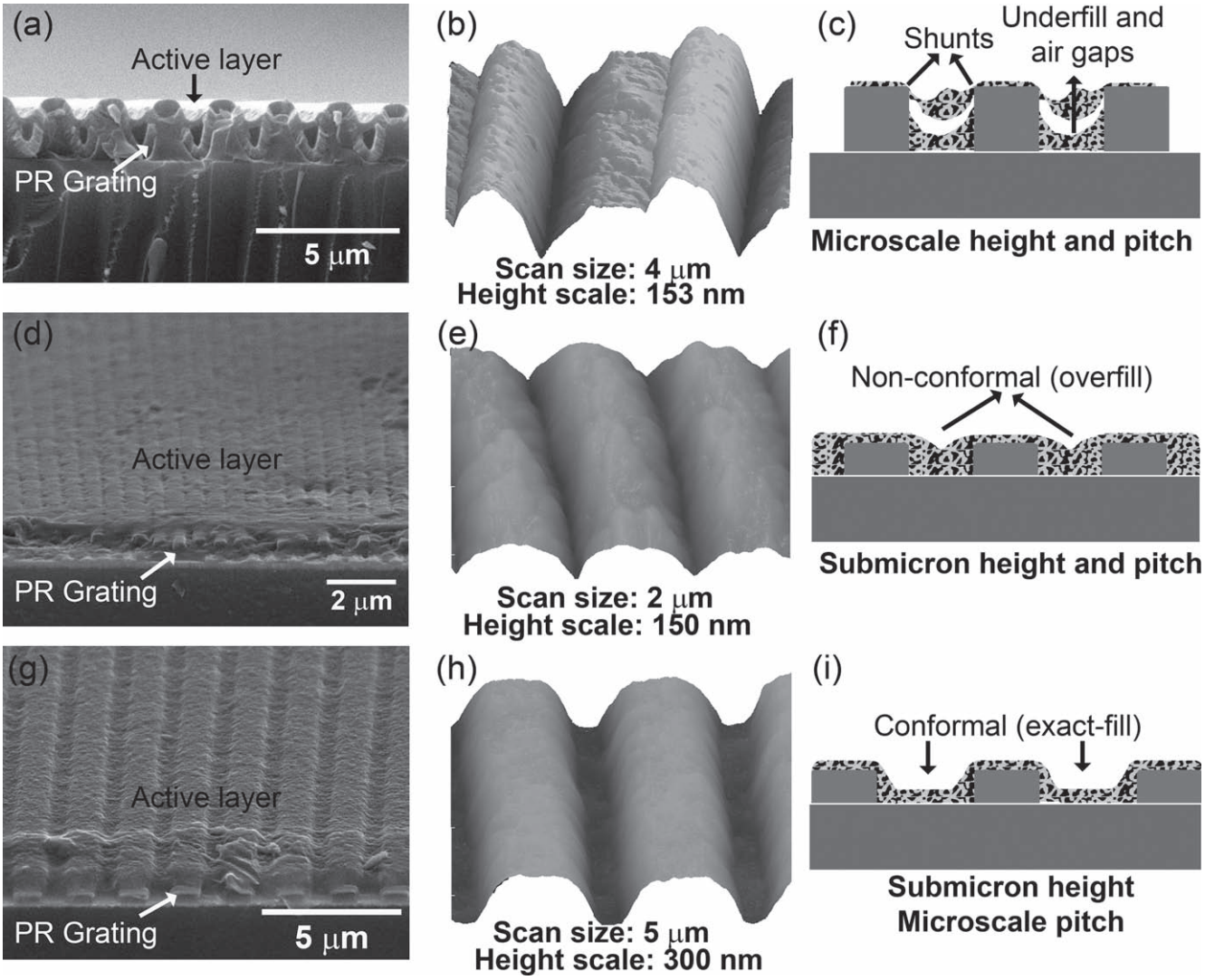

Figure 2. SEM (left), AFM (middle), and schematic (right) of P3HT:PCBM active-layer spin-coated on photoresist grating substrates of: (a–c) 2 μm pitch and 2 μm height; (d–f) 600 nm pitch and 300 nm height; and (g–i) 2 μm pitch and 300 nm height. Not shown in the schematics are the ITO and PEDOT:PSS layers, that were sputtered and spin-coated, respectively, before spin-coating the active-layer.

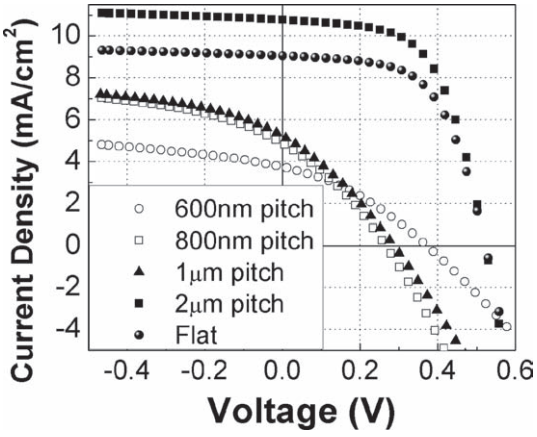

Figure 3. Photocurrent dependence on pitch of the 300 nm height grating based PV cells and the reference flat cell.

$$m\lambda = n_{active} p(\sin\theta_i + \sin\theta_d) \quad (1)$$

where m is the diffraction order, λ is the wavelength of incident light, n_{active} is the refractive index of the active-layer, p is the pitch of grating, and θ_i and θ_d are incidence and diffraction angles, respectively. A constant n_{active} was considered as 2 in the spectral wavelength range between 300 and 700 nm for simplification.[22] Then, in the case of normal incidence, for 600 nm < λ < 700 nm, m can take values of 0, ±1, ±2, ±3, ±4, ±5 and ±6, because sin $\theta_d \leq 1$ and p = 2 μm. Due to the higher order diffractions and their large diffraction angles in the grating cells, the zeroth order reflection intensity was reduced as was the total reflection, leading to increased path length and enhanced absorption of higher wavelength photons. The increased path length in the grating cell also results in some improvement in EQE for lower wavelength photons (400–500 nm), as evident in the distinct peaks

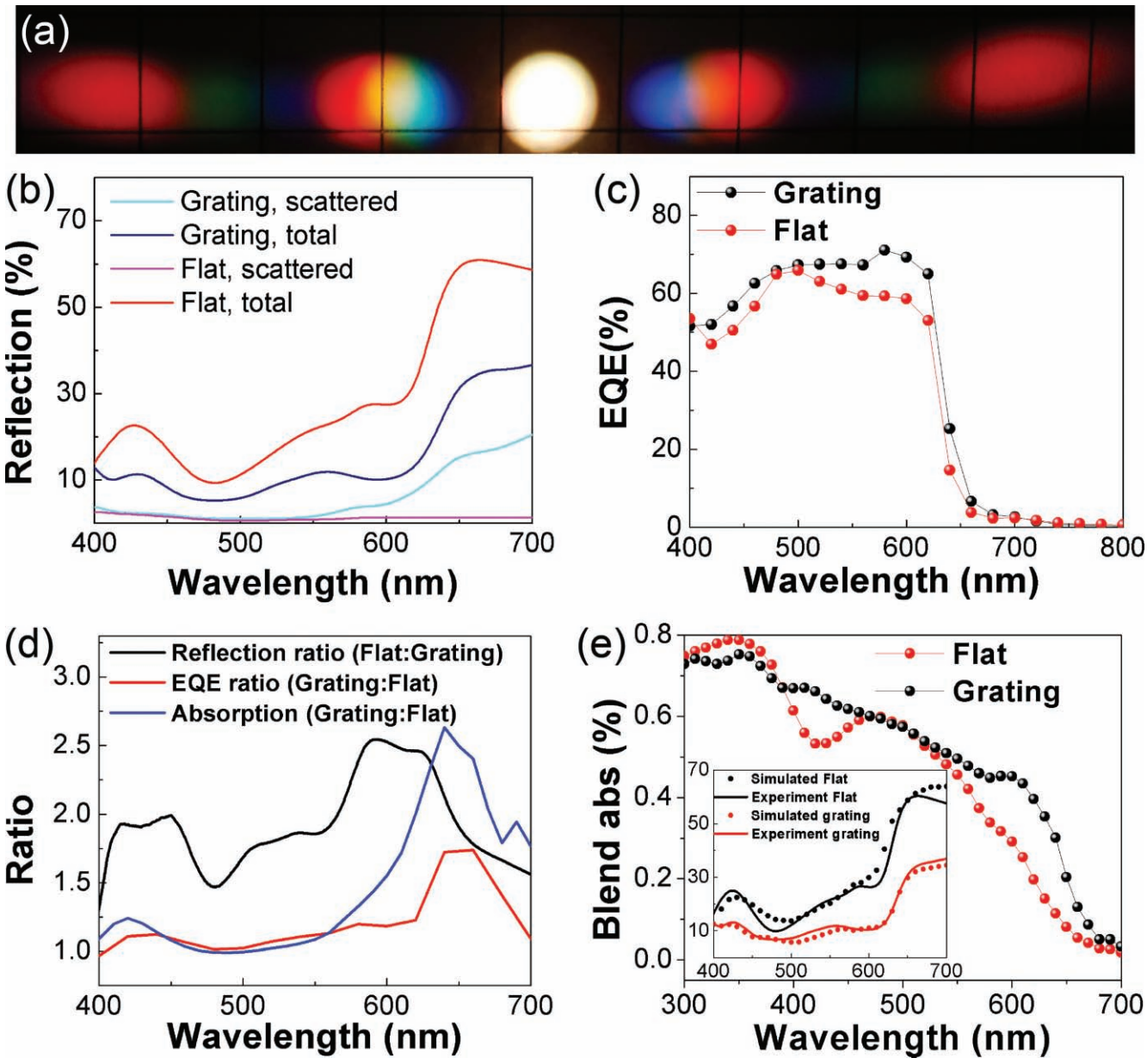

Figure 4. (a) Optical micrograph showing the spots of different diffraction modes when incident light on the grating cell is reflected and diffracted back from the Al cathode. (b–e) For the 2 μm pitch–300 nm height grating cell and the flat cell: (b) Total and scattered reflection measured at normal incidence; (c) EQE; (d) Reflection, simulated absorption and EQE ratios; and (e) Simulated active-layer absorption averaged over TE and TM polarizations. Inset in (e) shows polarization averaged experimental and simulated total reflection for the flat and the 300 nm height and 2 μm pitch grating cells.

in reflection, absorption and EQE ratios in this wavelength range (Figure 4d).

The aforementioned approximation of $A = 100–R$ is a measure of total absorption within the device, including within layers other than the P3HT:PCBM active-layer. For more precise determination of absorption in the active-layer, we performed simulations using the finite element model inbuilt in COMSOL MULTIPHYSICS, accounting for wavelength dependence of dielectric functions for materials. A good fit between the measured and the simulated total reflection at normal incidence is obtained for the 300 nm height and 2 μm pitch grating cell and flat cell, as shown in inset of Figure 4e. Simulated polarization averaged absorption in active-layer is shown in Figure 4e. In the visible range, the grating geometry shows higher absorption in the 400 nm to 450 nm wavelength regime. However, the most significant absorption improvement using the grating geometry is obtained at the band-edge of P3HT (~600 nm). Specifically, a 2.6-fold absorption enhancement is achieved at $\lambda = 640$ nm for grating cell, relative to the planar one. This conduces to an average 100% increase in absorption near the band edge ($600 \leq \lambda \leq 700$ nm). The EQE (Figure 4c) and EQE ratio (Figure 4d) follow the same trend as the simulated blend absorption

(Figure 4e), confirming that the improvement in device performance is indeed due to light-trapping, rather than increased device area or any electrical effect. For solar cells in a practical environment where sunlight can be quite diffused, it is also important to evaluate the absorption over a wide range of incident angles.[23] The grating based devices also showed advantage over the flat devices at higher incident angles of light (see supporting information).

In conclusions, we show that for sub-micrometer height topographies, it is possible to coat a conformal polymer film from solution if the pitch of the topography is few times higher, that is, larger than a micrometer. Realizing polymer PV cells on such topographies provides an efficient way to achieve light-trapping without compromising with electrical characteristics. Such P3HT:PCBM cells fabricated in our study showed 20% improvement in PCE relative to the flat control, owing to broadband light-trapping, especially at the band-edge where 100% average absorption increase was observed. Although we used spin-coating for the deposition of PV active-layer, but amenable topographical dimensions discovered in this study should also be relevant for implementing this light-management scheme using roll-to-roll coating techniques like gravure coating, upon some adaptation. An example of adaptation can be lateral acceleration and/or inversion of substrate upon the application of polymer solution. This can provide an external stimulus similar to what centrifugal force provides in the spin-coating process to enable the flow of solution over textured topographies and realization of conformal coatings.

Experimental Section

Photoresist gratings were made by laser interference holography with Lloyd's mirror setup on ITO coated glass slides. AZ-hir 1075 PR was spin coated on pre-cleaned ITO substrates (5-15 Ω/υ, Delta Technologies), prebaked in oven at 60 °C for 30 min, exposed by sinusoidal interference patterns made with Ar laser ($\lambda = 364$ nm), and then post baked at 110 °C for 1 min. It was then developed in MIF 300 developer for 1 minute followed by a rinse in distilled water. The period of pattern was changed by changing the angle of incidence, and height was changed by changing spin coating parameters. Although these PR gratings were made on ITO substrates, but to have better electrical connectivity of the photo active-layer with bottom ITO electrode, 120 nm ITO was sputtered on these PR gratings at 20 W RF power in Argon at room temperature (see supporting information for the reason behind choosing 120 nm thickness of sputtered ITO). Same thickness of ITO (120 nm) was sputtered on the commercial ITO coated glass slides to fabricate flat PV cells, for the sake of controlled comparison with the grating PV cells. The following procedure was kept same for the fabrication of flat and grating PV cells. A hole conducting film of PEDOT:PSS (CLEVIOS P VP AI 4083) was spin coated at 3000 rpm after treating the sputtered ITO layer with air plasma. The films were annealed at 120 °C for 10 min. The samples were then transferred inside the Ar atmosphere glove box. The P3HT:PCBM blend with 1:1 weight ratio was used. P3HT concentration was 17 mg/ml in dichlorobenzene. The blend active-layer was spin coated at 600 rpm for 60 s. After spin coating, the samples were allowed to dry slowly under a petri dish. Finally, Al (100 nm) electrode was deposited in a vacuum evaporator. I-V characterization was done using ELH Quartzline halogen lamp, the intensity of which was calibrated using a crystalline Si cell with a KG-5 filter. EQE measurements were also done using this lamp and a monochromator with a lock-in amplifier to eliminate background noise. The reference was a calibrated Si photodiode with known EQE spectra. Reflection measurements were performed using ocean optics setup with an integrating sphere.

Supporting Information

Supporting Information is available from the Wiley Online Library or from the author.

Acknowledgements

KS and SC thank Iowa Power Fund and Ames Laboratory seed funding for financial support. JMP and KMH thank Director for Energy Research, Office of Basic Energy Sciences. The Ames Laboratory is operated for the US Department of Energy by Iowa State University under contract no. DE-AC02-07CH11358.

Received: August 10, 2010
Revised: September 19, 2010
Published online: November 11, 2010

[1] G. Li, V. Shrotriya, J. S. Huang, Y. Yao, T. Moriarty, K. Emery, Y. Yang, *Nat. Mater.* **2005**, *4*, 864.
[2] J. Peet, J. Y. Kim, N. E. Coates, W. L. Ma, D. Moses, A. J. Heeger, G. C. Bazan, *Nat. Mater.* **2007**, *6*, 497.
[3] W. L. Ma, C. Y. Yang, X. Gong, K. Lee, A. J. Heeger, *Adv. Funct. Mater.* **2005**, *15*, 1617.
[4] L. Yongye, X. Zheng, X. Jiangbin, T. Szu-Ting, W. Yue, L. Gang, R. Claire, Y. Luping, *Adv. Mater.* **2010**, *22*, E135.
[5] H. Y. Chen, J. H. Hou, S. Q. Zhang, Y. Y. Liang, G. W. Yang, Y. Yang, L. P. Yu, Y. Wu, G. Li, *Nat. Photon.* **2009**, *3*, 649.
[6] S. H. Park, A. Roy, S. Beaupre, S. Cho, N. Coates, J. S. Moon, D. Moses, M. Leclerc, K. Lee, A. J. Heeger, *Nat. Photon.* **2009**, *3*, 297.
[7] J. Y. Kim, S. H. Kim, H. H. Lee, K. Lee, W. L. Ma, X. Gong, A. J. Heeger, *Adv. Mater.* **2006**, *18*, 572.
[8] H. Shah, A. Mohite, T. Bansal, B. Alphenaar, in *The American Physical Society March 2010 Meeting*, Vol. *55*, Portland, Oregon.
[9] P. Peumans, V. Bulovic, S. R. Forrest, *Appl. Phys. Lett.* **2000**, *76*, 2650.
[10] S. B. Rim, S. Zhao, S. R. Scully, M. D. McGehee, P. Peumans, *Appl. Phys. Lett.* **2007**, 91.
[11] M. Niggemann, M. Glatthaar, A. Gombert, A. Hinsch, V. Wittwer, *Thin Solid Films* **2004**, *451-52*, 619.
[12] M. Niggemann, M. Glatthaar, P. Lewer, C. Muller, J. Wagner, A. Gombert, *Thin Solid Films* **2006**, *511*, 628.
[13] C. Cocoyer, L. Rocha, C. Fiorini-Debuisschert, L. Sicot, D. Vaufrey, C. Sentein, B. Geffroy, P. Raimond, *Thin Solid Films* **2006**, *511*, 517.
[14] L. S. Roman, O. Inganas, T. Granlund, T. Nyberg, M. Svensson, M. R. Andersson, J. C. Hummelen, *Adv. Mater.* **2000**, *12*, 189.
[15] S. I. Na, S. S. Kim, J. Jo, S. H. Oh, J. Kim, D. Y. Kim, *Adv. Funct. Mater.* **2008**, *18*, 3956.
[16] D. H. Ko, J. R. Tumbleston, L. Zhang, S. Williams, J. M. DeSimone, R. Lopez, E. T. Samulski, *Nano Lett.* **2009**, *9*, 2742.
[17] G. Garcia-Belmonte, A. Munar, E. M. Barea, J. Bisquert, I. Ugarte, R. Pacios, *Org. Electron.* **2008**, *9*, 847.
[18] J. Zhu, C. M. Hsu, Z. F. Yu, S. H. Fan, Y. Cui, *Nano Lett.* **2010**, *10*, 1979.
[19] J. H. Lee, C. H. Kim, K. M. Ho, K. Constant, *Adv. Mater.* **2005**, *17*, 2481.
[20] W. H. Koo, S. M. Jeong, F. Araoka, K. Ishikawa, S. Nishimura, T. Toyooka, H. Takezoe, *Nat. Photon.* **2010**, *4*, 222.
[21] The calculated (with AM 1.5) short circuit current densities from EQE plots of 2 μm pitch-300 nm height grating and flat OPVs are 9.8 and 8.2 mA/cm^2 respectively, which are lower than the respective current densities measured under the lamp i.e. 11 and 9 mA/cm^2.
[22] F. Monestier, J. J. Simon, P. Torchio, L. Escoubas, F. Florya, S. Bailly, R. de Bettignies, S. Guillerez, C. Defranoux, *Sol. Energy Mater. Sol. Cells* **2007**, *91*, 405.
[23] K. S. Nalwa, S. Chaudhary, *Opt. Expr.* **2010**, *18*, 5168.